A reliability-based approach to the robustness of corroded RC structures

Eduardo S. Cavaco[a,b], Luis A. C. Neves[c], Joan R. Casas[d,*]

[a] *Civil Engineering Department, Universidade NOVA de Lisboa, Quinta da Torre, 2829-516, Monte da Caparica, Portugal*
[b] *CERIS - Civil Engineering Research and Innovation for Sustainability, Av. Rovisco Pais, 1 1049-001 Lisboa, Portugal*
[c] *Nottingham Transportation Engineering Centre (NTEC), Dept. of Civil Engineering, University of Nottingham, NG7 2RD Nottingham, United Kingdom*
[d] *Civil Engineering Department, Technical University of Catalunya, Modulo C1, Barcelona, Spain*

Abstract

Currently, decisions on infrastructural assets maintenance and repair, in particular on structures, are based, mostly, on the results of inspections and the resulting condition index, neglecting systems robustness, and, therefore, not making optimal use of the limited available funds. This paper presents a definition and a measure of structural robustness in the context of deteriorating structures, compatible with asset management systems for optimal maintenance and repair planning. The proposed index is used in defining the robustness of existing RC structures to rebar corrosion. Structural performance and the corresponding reliability index are assessed using combined advanced reliability and structural analysis techniques. Structural analysis explicitly includes deterioration mechanisms resulting from corrosion such as reinforcement area reduction, concrete cracking and bond deterioration.

*Corresponding author
Email address: `joan.ramon.casas@upc.edu` (Joan R. Casas)

The First Order Reliability Method, combined with a Response Surface algorithm, is used to compute the reliability index for a wide range of different corrosion levels, resulting in a fragility curve. Finally, structural robustness is computed and discussed based on the obtained results. Robustness comparison of different structures can then be used to determine structural types more tolerant to corrosion and these results can be used for maintenance and repair planning.
Keywords: Robustness, Reliability, Damage, Reinforced Concrete, Corrosion

1. Introduction

Maintaining safety and serviceability of existing structures and bridges by making better use of available resources is one of major challenges of transportation agencies in most developed countries since the number of structures reaching the design life-time is growing year after year [1]. Strategies, as giving priority to the poorest condition, are clearly insufficient as do not take advantage of structural robustness and tolerance to damage. Currently, decisions on maintenance and repair are reactive and based, mostly, on the results of visual inspection and the resulting condition index. The condition index is a convenient indicator of the deterioration of a structure, but provides little information regarding the structural safety, as neither the initial (intact) safety nor the impact of deterioration on safety is considered. Experience has shown that different structures can, for similar deterioration levels, present significantly different safety reductions and safety levels, with a dramatic effect on the need to repair and on the optimal allocation of funds in a network.

This paper presents a framework to assess robustness of structures under deterioration. Considering that a detailed safety assessment of every existing structure is impossible due to financial limitations and to the uncertainty related to the real deterioration, the robustness concept proposed herein can serve as an approximated measure of the mean loss in safety independent of the deterioration level for a given bridge type. The proposed robustness framework can then be combined with the bridge deterioration information to obtain a better indication of current and future safety loss due to deterioration and, therefore, to define an optimum maintenance policy. For instance, the robustness indicator may help the decision-maker to take a wise decision regarding the maintenance operations to be delivered on two bridges with equal or similar condition rating.

Although a robustness analysis is also complex, the robustness of similar structures is believed to be relatively uniform, allowing a classification of structures in a network based on the detailed analysis of a limited number of structural typologies. This classification can be used in conjunction with the observed or predicted condition state to define the need or urgency of maintenance, considering explicitly the structural properties of a particular structure. This allows a clear distinction between structures which, although presenting similar deterioration levels in specific main components, have very different safety levels as a result of different geometry or critical failure paths, among others.

Focus is also given to reinforced concrete structures (due to representativeness of this structural type worldwide) under reinforcement corrosion as this is one of the major causes of structural deterioration.

2. Structural robustness

Research on robustness has focused on extreme events, such as terrorist attacks. However, the concept can also be very useful in the context of structural aging and deterioration, in particular in the asset management field. Robustness of some structural types can be crucial to plan and design future infrastructures, requiring less repair and maintenance actions during service lifetime.

In what respects to corrosion of reinforced concrete structures, although the mechanisms responsible for rebar corrosion are relatively well known [2], the prediction of future deterioration is associated with very large uncertainty. For this reason, deterioration of reinforced concrete structures can be analyzed in a robustness framework, considering corrosion as unpredictable and assuming levels within a wide range. This approach is useful for both new and existing structures, as it indicates, on one hand, the structural designs less susceptible to corrosion and, on the other hand, the existing structures for which higher whole life repair costs can be expected.

Although robustness is a desirable property, a consensual definition and a framework to assess it still do not exist [3]. Significant work has been done, in particular under COST[1] Action TU-0601 - Robustness of Structures, but no unanimous methodology has yet been found.

Some authors suggest robustness to be a structural property [4, 5, 6, 7]

[1]COST - European Cooperation in the field of Scientific and Technical Research

while for others robustness depends also on the surrounding environment [8]. In this case, Robustness is a much broader concept, since it accounts with indirect consequences of failure which depend on several aspects such as social and economical. A deep discussion on the robustness concept can be found in [7].

In this paper the perspective of robustness being a structural property is adopted, in order to characterize the damage tolerance of existing structures to deterioration. The proposal of [7] is considered since it is sufficiently generic to be applied to most structural types and damage scenarios and can be applied in a probabilistic or deterministic framework. Robustness is defined as a structural property which measures the degree of structural performance remaining after damage occurrence. This relation can take many different forms, depending of the limit state (from service to ultimate limit state) that is adopted in the structural evaluation. Damage can vary from simple degradation to a more serious damage scenario as a local failure.

In order to assess robustness, it is fundamental to define a measure of structural performance f and a damage D causing performance decrease. The next step is to define the performance function of the damaged structure $f(D)$ for the complete damage spectrum. The maximum value of damage in the spectrum corresponds to the maximum expected loss of performance during service life. This is important when comparing robustness of different structural types, where the performance profile can be highly different as a function of the damage level or, alternatively, the service life. In the final step, both damage and performance indicator are normalized and the robustness indicator R_D is computed as follow:

$$R_D = \int_{D=0}^{D=1} f(x)dx \qquad (1)$$

For null robustness structures, a small level of damage produce a total loss of structural performance and vice-versa.

The proposed index, R_D, is a generalization of the proposals of [4, 6] and the damage based measure, $R_{d,int}$ proposed by [3], however with some advantages which appear to solve some of the limitations found in the referred robustness measures. The proposal of [4] is not suitable to deal with continuous damage, which is the case of reinforcement corrosion. This problem appears to be solved in the [6] proposal. Although this index considers continuous values for the damage variable, it results in different values for the robustness index, depending on the damage level. These problems have been solved by the proposed index, R_D, by considering normalized and continuous values for both structural performance and damage. Additionally, since all the damage domain is integrated, robustness is given by a unique value independently of the damage level. Thus, robustness may result similar for different structures even if one degrades continuously and the other reacts brittle. However, this can be surpassed if a probabilistic approach is used to measure the structural performance.

In this paper, the robustness of reinforced concrete structures subjected to corrosion is analyzed. Damage inflicted to the structure is considered to be the corrosion level on the reinforcement measured in terms of rebar weight loss percentage. The difficulties in defining a probabilistic model for hazard, in this case for corrosion, lead to the analysis under a range of different corrosion levels. This strategy has been used in seismic engineering for instance, where fragility curves resulting from exposing structures to different earthquakes intensities, have been used to characterize structural performance to seismic events. However the concept can be extended to a wide range of other hazards, as structural deterioration and in particular to reinforcement corrosion.

In this paper, structural performance is measured through the reliability index as this is a consistent measure of structural safety which takes uncertainty into account.

3. Corrosion of reinforced concrete structures

3.1. Corrosion process

When reinforced concrete is exposed to environmental conditions, steel bar corrosion and iron oxides formation are likely to occur due to the energetic potential of the iron-carbon alloy. The iron oxides resulting from the corrosion reaction do not have mechanical properties comparable to those of steel and exhibit volume increase which can go to seven times the original steel volume. The final result is the occurrence of several deteriorating mechanisms which lead to a deterioration of the structural capacity.

During the lifetime of a reinforced concrete structure two periods concerning corrosion can be distinguished [9]: the initiation period, respecting to the stage where reinforcement is protected by a thin oxide layer. Within this period corrosion takes place at a negligible rate and no deterioration effects are expected. The second phase, the propagation period, starts when concrete cover is contaminated and the passive oxide layer is destroyed. This results in increased corrosion rate and deterioration of the structure condition.

Steel depassivation occurs mainly due to concrete carbonation and chlorides contamination, typical of industrial and maritime environments, respectively. In the first case, corrosion is likely to occur uniformly, along steel bars length, while in the second case corrosion tends to be more localized and pronounced, also called pitting corrosion. In both cases several deterioration mechanisms are expected to aggravate the structure condition: reinforcement effective area reduction; ductility reduction of steel bars; concrete cracking and spalling of concrete; bond degradation between steel bars and surrounding concrete. The influence of these mechanism on the structural behavior depends on several factors such as type of corrosion, reinforcement ratio, concrete strength, loading, cross section geometry, among others [10]. In general, steel bars effective area and ductility reduction are of more concern in cases of localized or pitting corrosion [11, 12], while concrete cracking and spalling and debonding effect play a more deteriorating role in cases of general corrosion [13, 14, 15, 16].

Ductility reduction of steel bars is partly due to a chemical transformation of the steel occurring during corrosion process, known as *hydrogen embrittlement* [17, 18] and partly due to a localization phenomenon resulting from non uniform corrosion [19]. The latter can explain the reason behind ductility reduction of steel bars have been considered specially concerning in cases of pitting corrosion. In these cases however, concrete cracking and spalling and debonding of reinforcement are, in general, not critical, as steel bars can be anchored in less corroded and non cracked zones [20]. However, if corrosion attacks all bar length, spalling of concrete cover is likely to occur and loss of bond between steel bars and concrete, compromising the composite behavior of both materials, is expected. [21] have concluded the effects of localized and generalized corrosion to be potentially more hazardous for bending ultimate and service limit states of highway bridges, respectively. However, it must be noted that the authors have assumed perfect anchorage of reinforcement in the abutments. Even if hooks are provided at reinforcement ends, anchorage can be greatly impaired by the existence of lapped joints reinforcement [22]. Additionally, it must be noted that corrosion rate is usually increased in zones of reinforcement concentration or where it is bent. According to [13] and [14] reinforcement debonding is the main cause of impaired flexural behavior, if corrosion is found to be generalized and uniform.

This paper addresses generalized and uniform corrosion. Localized and pitting corrosion stay outside the scope. From this stage onwards, and for sake of simplicity, only the effects of concrete cracking and spalling, debonding of steel bars and reinforcement effective area reduction will be considered. Reinforcement impaired ductility and reduction of steel strength, including the spatial variability of corrosion, are not considered herein, although it is recognized, and as suggested by [11, 12, 23], that these are factors of paramount importance in cases of localized corrosion, which is not the present case.

3.2. Methodology

As discussed in the previous section, to adequately model the effects of generalized corrosion it is necessary to take into account some undesirable consequences of the oxidation process of rebars, including reinforcement net area reduction and expansion due to corrosion products accumulation. This last phenomenon leads to damage, cracking and splitting of the surrounding concrete and degradation of steel-concrete bond, responsible for stress transfer between both materials.

In order to model all these effects, an advanced Finite Element methodology was used coupled with advanced constitutive models for modeling materials. Its capability to reproduce the behavior of corroded reinforced concrete was demonstrated by comparing numerical results with results obtained experimentally [24]. The methodology employed considers a two-step analysis. In the first step a finite element analysis of the structure cross section is carried out, simulating the formation and accumulation of corrosion products as an expansion of steel bars. In this phase, steel bars are modeled using a linear elastic law and are coupled to concrete through an interface model that regulates the shear stress transference between the two materials. For sake of simplicity, corrosion is considered to attack uniformly around the bar perimeter, although it is known that corrosion is more pronounced in outer part of the steel bar. For concrete, an isotropic continuum damage model is used enriched with kinematics provided by the strong discontinuities theory [25]. The combination of these two approaches, for modeling concrete behavior, allows the simulation of crack development caused by corrosion and expansion of rebars.

In the second step, results obtained during the cross section analysis are then used to build a 2D structural model of the corroded structure used to assess the impaired structural capacity. Reinforced concrete is modeled by means of a composite material constituted by a matrix, representing concrete, mixed with long fibers which represent steel bars, as proposed by [26]. This is the main difference from the modeling strategy proposed by [24]. Whereas

[24] used a mesoscopic approach for the 2D longitudinal model, using different finite elements for concrete, reinforcing bars and interface. In the homogenized model used herein, a unique composite finite element is enriched to reproduce the composite behavior of all the components. As an advantage, the homogenized model requires much less computational resources, due to the smaller size of the numerical model. This is an important aspect in this case, since a large number of different analyzes are required to perform the fragility curves. Additionally, the homogenized model seems to reproduce better the global structural behavior since the interface between concrete and steel bars is implicitly considered. In the mesoscopic approach, bond effect is reproduced using interface elements. In this manner, results can be affected by the mesh size, usually resulting in a less stiff global behavior.

3.3. Cross section analysis

This section depicts results obtained in the first step of the corrosion analysis methodology, obtained for a rectangular section (0.20m×0.40m) with mean values properties of a C30/37 concrete and 2ϕ10 and 2ϕ20 reinforcement steel bars (S400 grade) placed at the upper and bottom section surfaces, respectively. Corrosion was simulated considering a volumetric expansion of steel bars, with similar penetration rates on both bars. Resulting iron oxides, as suggested by [27], were considered incompressible and to occupy twice the initial iron volume. Figure .1 shows the effect of corrosion at a cross section level. Figure .1 (a) shows damage map, d, on concrete due to expansion of steel bars for a corrosion penetration depth, $X = 0.5$mm, which correspond to an area percentage lost of $X_{P1} = 10\%$ and $X_{P2} = 20\%$ for bottom and top reinforcement, respectively. Damage $d = 1$ means concrete had lost all strength and cracking is eminent. Figure .1 (b) shows the corresponding iso-displacement lines which concentration indicates crack development as shown in Figure .1 (c).

[Figure 1 about here.]

Figure .2 shows width evolution of cracks (a) to (e) as corrosion increases. Cracks (a) and (e) are those reaching the range of visible cracks ([0.1-0.2]mm) for X_{P_1} and X_{P_2} equal to 1% and 2%, respectively, therefore consistent with experimental results [10]. Figure .2 shows that, for corrosion X_{P_1} and X_{P_2} above 5% and 10%, respectively, cracks width increase linearly and no additional cracks were detected. This allow the definition of the effective concrete cross section as shown in Figure .1 (d). For sake of simplicity, corrosion of transverse reinforcement was neglected [21], although it is recognized, on one hand the respective positive confinement effect, and on the other hand the additional negative contribution for the cross section deterioration.

[Figure 2 about here.]

3.4. Structural Analysis

Results obtained for the cross section analysis were used to build a 2D structural model of the corroded structure. A simply supported 5.0m span beam was used to illustrate the proposed methodology. Reinforced concrete was modeled by means of a composite material constituted by a matrix, representing concrete, mixed with long fibers which represent steel bars, as proposed by [26]. Three types of composite material needed to be considered (see Figure .3): concrete cover (unreinforced plane concrete); concrete on the beam's web, transversely reinforced; and concrete surrounding flexural bars, longitudinally reinforced. As for the cross section analysis, and in order to be able to model crack development, in the longitudinal model the finite elements were also enriched with the strong discontinuities kinematics [25], and for concrete the isotropic continuum damage model was adopted [28].

[Figure 3 about here.]

For the embedded fibers, the objective was to simultaneously model reinforcement behavior and debonding effect, resulting from corrosion. In order to achieve such goal, the slipping-fiber model proposed by [26] was adopted, which considers slipping-fiber ϵ^f strain as the sum of the fiber mechanical deformation and the deformation of interface.

[Figure 4 about here.]

Assuming a two-component serial system constituted by the fiber and the interface, the corresponding slipping-fiber stress σ^f is identical to the stress of each component. On both cases the stress-strain relation can be obtained via an one-dimensional elasto-plastic hardening/softening model. The resulting constitutive behavior, for the slipping-fiber, is also an elasto-plastic model with the following characteristics:

$$\sigma_y^f = min(\sigma_y^d, \sigma_y^i) \tag{2}$$

$$E^f = \frac{1}{\frac{1}{E^d} + \frac{1}{E^i}} \tag{3}$$

in which E^d and σ_y^d are the steel Young's modulus and yield stress, respectively, E^i is the interface elastic modulus and σ_y^i is the interface bond limit stress. Regard that, when $E^i \to \infty$ and $\sigma_y^d < \sigma_y^i$, the system provides only the mechanical behavior of the fiber, reproducing a perfect adhesion between concrete and reinforcement bars.

For the slipping-fiber model characterization, pullout tests can be performed in order to assess the required parameters. In this paper, for the uncorroded state, perfect adhesion between steel bars and concrete is considered and a rigid-plastic behavior for the interface is adopted. This hypothesis may be considered acceptable since it is considered that the anchorage lengths are respected and only ultimate limit states related to structural capacity are under analysis. For corroded states, the bond limit stress σ_y^i was considered lower than the reinforcement yielding stress σ_y^d, and depending on the corrosion level X_P. This means that perfect adhesion it is not valid for the corroded states, as suggested by several researchers [29, 14, 15, 30, 16]. The steel yield strength was considered not affected by corrosion, although reductions have been documented, in particular in cases of localized corrosion. In order to characterize bond strength reduction as a function of the corrosion level the *M-pull* model proposed by [31] was adopted. This is an empirical model, based on several author's experimental tests (see Figure .5), thus the following results must be watched carefully. The *M-pull* gives the normalized bond strength reduction depending on the corrosion level:

$$\frac{\sigma_y^i(X_p)}{\sigma_y^i(X_p = 0)} = \begin{cases} 1.0 & if \;\; X_p \leq 1.5\% \\ 1.192 \cdot e^{-0.117 X_p} & if \;\; X_p > 1.5\% \end{cases} \tag{4}$$

For sake of simplicity, bond degradation was considered uniform around the steel bars perimeter.

[Figure 5 about here.]

To build the 2D structural longitudinal model of the deteriorated structure, it was necessary to import the results obtained for the cross section corrosion analysis (see Figure .6 (a)). As referred, special attention was given to crack pattern, *i.e.*, when a crack crossed two cross section faces, the smaller section part was considered disconnected from the section core (see Figure .6 (b)) and then, for simplicity, considered with damage $d = 1$ (see Figure .6 (c)). In this case, and as observed in the previous section, for advanced corrosion stages, concrete corners at both beam's top and bottom tended to split from the section core. The next step was to divide the cross section into thin horizontal slices and compute the average damage, d, for each slice (see Figure .6 (d)). Finally the damage values for each slice, as shown in Figure .6 (e), were projected on the 2D longitudinal structural model (see Figure .6 (f)) defining the deteriorated structure.

[Figure 6 about here.]

4. Reliability Analysis

As previously referred, the reliability index, β, is the structural performance indicator chosen to assess robustness since it is a consistent measure of safety. However, the reliability of a corroding existing structure is a time-dependent problem, which can be expressed by the following equation:

$$P_f(t) = \int_{G[X(t)]} f_{X(t)}[X(t)]dx(t) \tag{5}$$

where $P_f(t)$ is the instantaneous probability of failure at time t, $X(t)$ is the random variables vector, $G[X(t)]$ is the limit state function and $f_{X(t)}$ the joint probability density function of the random variables. The instantaneous probability of failure can be integrated over an interval of time, $[0;t]$, resulting in the probability of failure over that time period, $P_f(0,t)$. The random variables, $X(t)$, are time dependent and, thus, so is $P_f(t)$. The time t at which the limit state function, $G[X(t)]$, becomes zero is denoted time-to-failure and equation (5) correspond to a first-passage-probability, assessed with the out-crossing theory [32]. Time-integrated approaches for solving equation (5) are much simpler, as lifetime maximums distributions for loads are used as presented in equation (6)

$$P_f(0,t) = P\Big(R(t) \leq S_{max}(t)\Big) \tag{6}$$

where $R(t)$ is resistance and $S_{max}(t)$ is the maximum load effect for the time period $[0;t]$. However, as resistance is also time dependent, decreasing with deterioration, it is extremely unlikely that the maximum load effect coincides with the time of minimum resistance. By dividing structure lifetime into n limited time periods, for which resistance can be considered as time invariant, it is possible to approach the first-passage problem by equation (7):

$$P_f(0,t) = 1 - P\Big(R_1 \geq S_{max,1} \cap R_2 \geq S_{max,2} \cap ... \cap R_n \geq S_{max,n}\Big) \tag{7}$$

where R_i respect to resistance at time interval $[t_{i-1};t_i]$, considered as constant, and $S_{max,i}$ is the maximum load effects within the same period. Despite the independence of $S_{max,i}$ between time periods, the subset of events presented in equation (7) still show some dependency as a result of the correlation between remaining involved variables. Establishing an analogy between different time periods and structural members of serial system, the probability of failure in (7) can finally be approached by the narrow reliability bounds proposed by [33].

Thus, if relative short time periods are considered, attending to the corrosion rate, the probability of failure, given a certain level of corrosion, can be considered approximately as time-independent. The corresponding reliability index, β, is therefore used herein as the time-independent performance indicator and equation (1) results in:

$$R = \int_0^1 \frac{\beta(X_P = x)}{\beta(X_P = 0)} dx \tag{8}$$

Under severe deterioration, negative reliability indices might occur, meaning the structure is very likely to fail. Such high risk will significantly decrease the robustness index, indicating the high potential consequences of deterioration. In order to compute the reliability index, the response surface method, RSM, is used to obtain an explicit approach for the structural response to allow the First Order Reliability Method, FORM, to be used [34, 35]. To depict the proposed methodology, the simply supported beam analyzed in the previous section is being used and considered to support a 0.075m depth and 1.25m wide concrete deck for pedestrians.

The number of random variables considered in this study needed to be restricted to the most fundamental, due to demanding reliability analysis, sophisticated numerical models, and limited computational resources. Table .1 shows the distributions and parameters of the six random variables considered as uncorrelated. The statistical properties of concrete [36, 37] and reinforcement bars have been considered. Live load is the result of people concentration and modeled through a exponential distribution with a 98% quartile of $7.0kN/m^2$ for the maximums distribution in a reference period of 50 years. This results in an exponential rate parameter, λ, of 1.1 and a mean value of $0.90kN/m^2$ for an annual occurrence rate. Thus the probability of failure to be computed will respect to the period of 1 year, and for the usual corrosion rates, the resistance of the deteriorating structure can be considered as constant. The width of the deck (1.25m) was considered on the surface loads.

[Table 1 about here.]

The limit state function, G, is defined as the resistance, R, minus the acting load, S, due to self weight and live load. The resistance is considered as the maximum uniform load that could be applied to structure until its failure in bending either defined by the steel bars yielding or the concrete crushing. The load effect, S, can be obtained through equation (9)

$$S = \theta_E \times \left[A_c^{beam} g + W \left(d_c^{slab} g + q\right)\right] \tag{9}$$

where W is the deck width equal to $1.25m$. A_c^{beam} and d_c^{slab} are the beam cross section and the slab depth, respectively. The resistance can be computed through equation 10:

$$R = \theta_R \times R\left(f_c, f_y, X_P\right) \tag{10}$$

where $R\left(f_c, f_y, X_p\right)$ is the resistance obtained through the corrosion analysis methodology described previously, and explicitly approached by a response surface defined for each design point, d_P.

5. Discussion

5.1. Reliability analysis

Figure .7 shows the reliability index, $\beta(X_P)$, and the respective failure probability, $P_f(X_P)$, evolution with the corrosion level, X_P. The reliability of the intact structure is 3.5 decreasing significantly as corrosion increases, specially in the first 15% of reinforcement area lost. For corrosion levels ranging from 15% to 40%, safety reduction is much less significant, and from this stage onwards almost negligible. The residual reliability is 0.41 attained for 60% of area lost.

Figure .7 also shows two additional fragility curves: $\beta(X_P)^*$, where the debonding effect has been neglected; and $\beta(X_P)^{**}$, where only reinforcement area reduction has been considered. The comparison between $\beta(X_P)$, $\beta(X_P)^*$ and $\beta(X_P)^{**}$ shows that safety reduction due to reinforcement area reduction is almost linear until corrosion reach about 80%. From this stage onwards, the effective reinforcement area is below the minimum required to avoid structural failure immediately after flexural cracks initiation. Cracking effect is more significant for corrosion above 80%, as from this stage onwards flexural strength is provided by the plain concrete section, which in this case is deteriorated as shown in Figure .1 (d).

[Figure 7 about here.]

5.2. Robustness assessment

Figure .8 shows the normalized performance obtained through the ratio between the reliability of the corroded structure and the intact one, as a function of the normalized damage, in this case considered as the corrosion level on bottom reinforcement. The maximum damage is limited to 50%, as for existing structures such level of deterioration would trigger a repair action and considering more advanced corrosion levels is clearly unrealistic.

[Figure 8 about here.]

Robustness computed according to (8) results in $R = 28\%$, showing that tolerance to generalized corrosion is relatively low and safety reduction should always be a concern. The mean normalized performance reduction is therefore 72%. This is a result of the lack of redundancy of a simply supported beam, but also of the absence of a second layer of bottom reinforcement less affected by corrosion.

Computing robustness of the remaining cases presented in Figure .7, results in $R^* = 75\%$ and $R^{**} = 82\%$ if debonding and debonding including cracking have been neglected, respectively. Establishing the difference between the computed robustness indicators (Δf), provides the relative importance of each deteriorating mechanism for the lack in robustness. It results that debonding effect is the main cause of structural deterioration producing a mean safety reduction $\Delta f^1 = 47\%$, followed by reinforcement area lost and then cracking, causing a mean performance reduction of $\Delta f^3 = 18\%$ and $\Delta f^2 = 7\%$, respectively (see Figure .8).

5.3. Decision making based on robustness

Figure .9 shows the beam time-dependent probability of failure $P_f(0,t)$, referred to the time period $[0,t]$, and considering a corrosion progression of 1% annually. The initiation period has been neglected and the time $t = 0$ respects to the onset of corrosion. The lower and the upper bounds of the probability of failure resulted very narrow and overlapped in Figure .9 as weak dependency was found between different time periods. Figure .9 also shows the time-dependent probability of failure for a similar beam but considered fully protected against corrosion, $P_f(0,t)^{***}$. The comparison between the unprotected and protected beam shows the impact of corrosion on the time-dependent safety indicating the former to be a case of concern, requiring premature intervention. The probability of failure is approximately the same within the periods of 5 and 50 years, for the unprotected and protected beam, respectively. Figure .9 also shows the time-dependent probability of failure when neglecting debonding effect, $P_f(0,t)^*$, and considering only the effect of reinforcement area reduction $P_f(0,t)^{**}$. As mentioned, debonding is the major cause for impaired robustness thus with major impact on the time-dependent probability of failure.

[Figure 9 about here.]

Similarly, a longer time between periodic inspections could be adopted depending on robustness. Figure .10 shows the time-dependent probability of failure, for the same cases of Figure .9, given the observed corrosion level at the inspection time and within the period of 3 years $P_f(3y|X_P)$. For exemplification proposes, the mean time between periodic inspections was considered herein equal to 3 years. As observed, the probability of failure within the time between inspections is constant for the beam protected against corrosion due to full robustness. For the unprotected beam, the probability of failure increases with the corrosion degree. Therefore a reduction of the time between inspections is required over the beam lifetime.

[Figure 10 about here.]

6. Conclusions

In this work, a probabilistic framework for the evaluation of structural robustness of structures, subject to continuous damage, is presented. In this framework, damage is defined in terms of an unpredictable continuous variable, making this robustness index particularly suitable for structural management systems allowing the analysis and comparison of different structural types with the final objective of defining those requiring more and prior maintenance.

The proposed robustness index can be used to estimate the need to repair a structure when damage is identified, since it provides an estimate of current and future structural safety. However, the inclusion of this index in existing management systems will require a calibration process, including a large pool of typical structures, where the condition index and the robustness index are related with the remaining time before a safety threshold is reached.

The results obtained showed the ability of the proposed index to characterize the robustness of a structure, from a structural viewpoint, in a single indicator, independently of the structural safety of the undamaged structure. Robustness of the presented example resulted in 28% which shows the structure tolerance to generalized reinforcement corrosion. The mean performance lost is 72% of which 47%, 18% and 7% are caused by bond deterioration, reinforcement area reduction and concrete cover cracking, respectively. The comparison with a similar beam but fully robust (due to a corrosion protection), shows that the unprotected beam, thus less robust, requires sooner maintenance and shorter periods between periodic inspections. For the sake of simplicity in introducing the concept of robustness index, the example presented in this paper corresponds to a single simply-supported beam. However, it is known that in statically indeterminate structures damage effects include a redistribution of internal forces. How this redistribution affects the final value of robustness because of redistribution of stresses and activation of alternative loading paths, is the subject of future research.

Acknowledgments

The authors would like to acknowledge Cost Action TU-0601, Fundação para a Ciência e Tecnologia scholarship SFRH/BD/45799/2008 and Research Project PTDC/ECM-COM/2911/2012, CERIS - Civil Engineering Research and Innovation for Sustainability, and the Spanish Ministry of Education, Research Project BIA2010-16332.

References

[1] A. Strauss, R. Wendner, D. M. Frangopol, K. Bergmeister, Influence line- model correction approach for the assessment of engineering structures using novel monitoring techniques, Smart Structures and Systems 9 (1) (2012) 1–20, 00010. doi:10.12989/sss.2012.9.1.001.
URL

[2] K. Vu, M. Stewart, Structural reliability of concrete bridges including improved chloride-induced corrosion models, Structural safety 22 (4) (2000) 313–333.

[3] U. Starossek, M. Haberland, Approaches to measures of structural robustness, Structure and Infrastructure Engineering 7 (7-8) (2011) 625–631.

[4] D. M. Frangopol, J. P. Curley, Effects of damage and redundancy on

structural reliability, Journal of Structural Engineering 113 (7) (1987) 1533–1549.

[5] N. Lind, A measure of vulnerability and damage tolerance, Reliability engineering & systems safety 48 (1) (1995) 1–6.

[6] F. Biondini, S. Restelli, Damage propagation and structural robustness, in: Life-Cycle Civil Engineering: Proceedings of the International Symposium on Life-Cycle Civil Engineering, IALCCE'08, Varenna, Lake Como, Taylor & Francis, 2008, p. 131.

[7] E. S. Cavaco, J. R. Casas, L. A. Neves, A. E. Huespe, Robustness of corroded reinforced concrete structures–a structural performance approach, Structure and Infrastructure Engineering 9 (1) (2013) 42–58.

[8] J. Baker, M. Schubert, M. Faber, On the assessment of robustness, Structural Safety 30 (3) (2008) 253–267.

[9] R. Melchers, C. Li, W. Lawanwisut, Probabilistic modeling of structural deterioration of reinforced concrete beams under saline environment corrosion, Structural Safety 30 (5) (2008) 447 – 460. doi:DOI: 10.1016/j.strusafe.2007.02.002.
URL

[10] F. i. d. b. fib, Bond of Reinforcement in Concrete: State-of-art Report, Bulletin (Fédération internationale du béton), International Federation for Structural Concrete, 2000.
URL

[11] M. G. Stewart, Spatial variability of pitting corrosion and its influence on structural fragility and reliability of rc beams in flexure, Structural Safety 26 (4) (2004) 453 – 470. doi:DOI: 10.1016/j.strusafe.2004.03.002.

[12] M. G. Stewart, A. Al-Harthy, Pitting corrosion and structural reliability of corroding rc structures: Experimental data and probabilistic analysis, Reliability Engineering & System Safety 93 (3) (2008) 373 – 382, probabilistic Modelling of Structural Degradation. doi:DOI: 10.1016/j.ress.2006.12.013.

[13] A. Almusallam, A. Al-Gahtani, A. Aziz, F. Dakhil, et al., Effect of reinforcement corrosion on flexural behavior of concrete slabs, Journal of materials in civil engineering 8 (1996) 123.

[14] P. Mangat, M. Elgarf, Flexural strength of concrete beams with corroding reinforcement, ACI Structural Journal 96 (1).

[15] R. Al-Hammoud, K. Soudki, T. H. Topper, Bond analysis of corroded reinforced concrete beams under monotonic and fatigue loads, Cement and Concrete Composites 32 (3) (2010) 194–203, 00025. doi:10.1016/j.cemconcomp.2009.12.001.
URL

[16] A. Kivell, A. Palermo, A. Scott, Corrosion Related Bond Deterioration and Seismic Resistance of Reinforced Concrete Structures, in: Structures Congress 2012, American Society of Civil Engineers, 2012, pp. 1894–1905, 00001.
URL

[17] R. Schroeder, I. Müller, Stress corrosion cracking and hydrogen embrittlement susceptibility of an eutectoid steel employed in prestressed concrete, Corrosion science 45 (9) (2003) 1969–1983.

[18] J. Woodtli, R. Kieselbach, Damage due to hydrogen embrittlement and stress corrosion cracking, Engineering Failure Analysis 7 (6) (2000) 427–450.

[19] R. Palsson, M. Mirza, Mechanical response of corroded steel reinforcement of abandoned concrete bridge, ACI Structural journal 99 (2).

[20] J. Cairns, Z. Zhao, Behaviour of concrete beams with exposed reinforcement, in: Proceedings of the Institution of Civil Engineers: Structures and Bridges, Vol. 99, 1993.

[21] D. V. Val, M. G. Stewart, R. E. Melchers, Effect of reinforcement corrosion on reliability of highway bridges, Engineering Structures 20 (11) (1998) 1010 – 1019. doi:DOI: 10.1016/S0141-0296(97)00197-1.
URL

[22] Y. Murakami, A. Kinoshita, S. Suzuki, Y. Hukumoto, H. Oshita, Influence of lapped splices on residual flexural behavior of rc beams with corrosion of reinforcement, Concrete Research and Technology 17 (1).

[23] M. G. Stewart, Q. Suo, Extent of spatially variable corrosion damage as an indicator of strength and time-dependent reliability of rc beams, Engineering Structures 31 (1) (2009) 198 – 207. doi:DOI: 10.1016/j.engstruct.2008.08.011.

[24] P. Sánchez, A. Huespe, J. Oliver, S. Toro, Mesoscopic model to simulate the mechanical behavior of reinforced concrete members affected by corrosion, International Journal of Solids and Structures 47 (5) (2010) 559 – 570. doi:DOI: 10.1016/j.ijsolstr.2009.10.023.

[25] J. Oliver, A. Huespe, M. Pulido, E. Chaves, From continuum mechanics to fracture mechanics: the strong discontinuity approach, Engineering Fracture Mechanics 69 (2) (2002) 113–136.

[26] J. Oliver, D. Linero, A. Huespe, O. Manzoli, Two-dimensional modeling of material failure in reinforced concrete by means of a continuum strong discontinuity approach, Computer Methods in Applied Mechanics and Engineering 197 (5) (2008) 332–348.

[27] F. Molina, C. Alonso, C. Andrade, Cover cracking as a function of rebar corrosion: Part 2numerical model, Materials and Structures 26 (9) (1993) 532–548.

[28] J. Oliver, M. Cervera, S. Oller, J. Lubliner, Isotropic damage models and smeared crack analysis of concrete, in: Second International Conference on Computer Aided Analysis and Design of Concrete Structures, Vol. 2, 1990, pp. 945–958.

[29] A. Almusallam, A. Al-Gahtani, A. Aziz, Effect of reinforcement corrosion on bond strength, Construction and Building Materials 10 (2) (1996) 123–129.

[30] H. Yalciner, O. Eren, S. Sensoy, An experimental study on the bond strength between reinforcement bars and concrete as a function of con-

crete cover, strength and corrosion level, Cement and Concrete Research 42 (5) (2012) 643–655, 00038. doi:10.1016/j.cemconres.2012.01.003.
URL

[31] K. Bhargava, A. Ghosh, Y. Mori, S. Ramanujam, Corrosion-induced bond strength degradation in reinforced concrete-analytical and empirical models, Nuclear Engineering and Design 237 (11) (2007) 1140–1157.

[32] R. E. Melchers, Structural reliability analysis and prediction, John Wiley & Son Ltd, 1999.

[33] O. Ditlevsen, Narrow reliability bounds for structural systems, Journal of structural mechanics 7 (4) (1979) 453–472.

[34] C. Bucher, U. Bourgund, A fast and efficient response surface approach for structural reliability problems, Structural safety 7 (1) (1990) 57–66.

[35] H. M. Gomes, A. M. Awruch, Comparison of response surface and neural network with other methods for structural reliability analysis, Structural Safety 26 (1) (2004) 49–67, 00205. doi:10.1016/S0167-4730(03)00022-5.
URL

[36] T. Zimmermann, D. Strauss, A. andLehký, D. Novák, Z. Kersner, Stochastic fracture-mechanical characteristics of concrete based on experiments and inverse analysis, Construction and Building Materials 73 (2014) 535–543, 00005. doi:10.1016/j.conbuildmat.2014.09.087.
URL

[37] A. Strauss, T. Zimmermann, D. Lehký, D. Novák, Z. Kersner, Stochastic fracture-mechanical parameters for the performance-based design of

concrete structures, Structural Concrete 15 (3) (2014) 380–394, 00010. doi:10.1002/suco.201300077.
URL

List of Figures

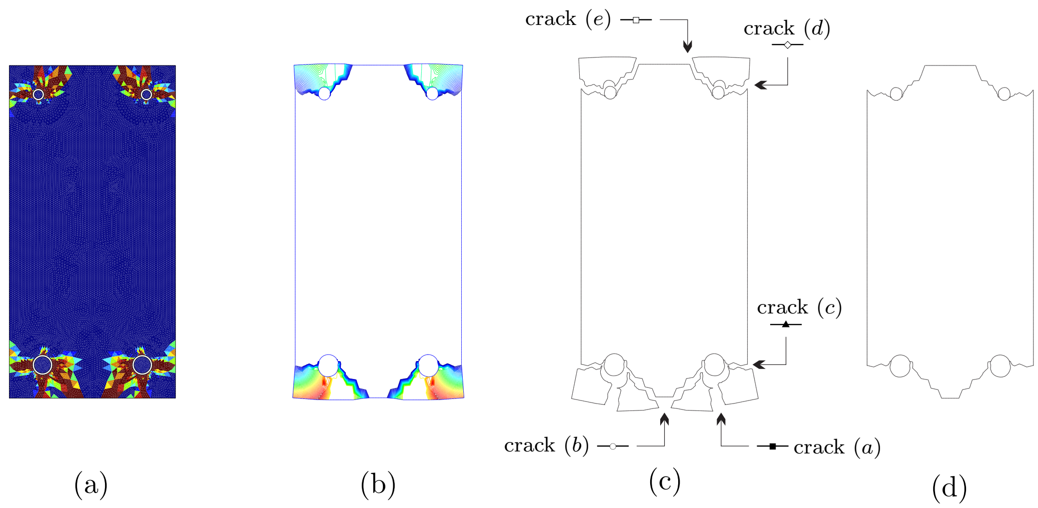

Figure .1: Damage and cracking on beam's cross section due to steel bar expansion. (a) Damage d, for $X_{P_1} = 10\%$, $X_{P_2} = 20\%$; (b) Iso-displacement contour lines; (c) Cracking pattern; (d) Effective cross section.

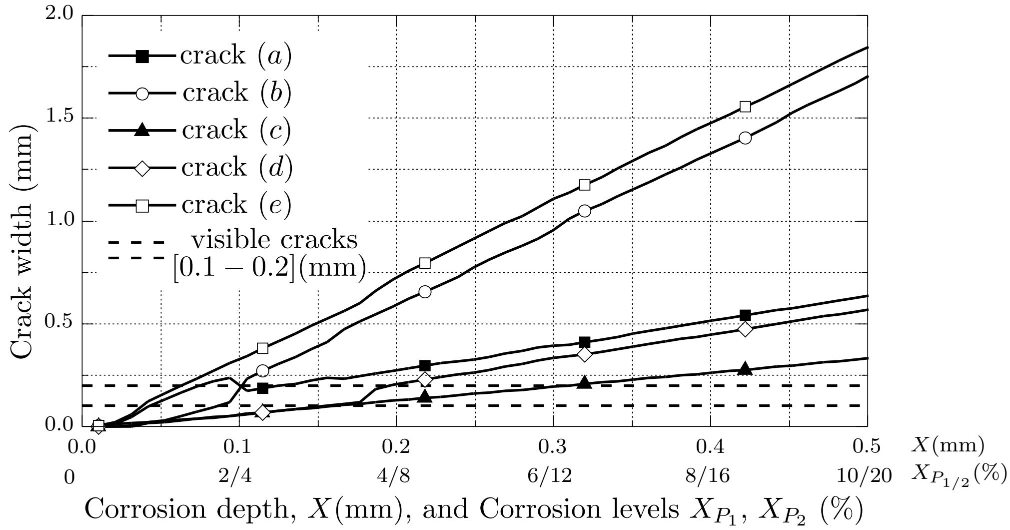

Figure .2: Cross section cracks width as a function of the corrosion depth, X, and levels, X_{P_1} and X_{P_2}

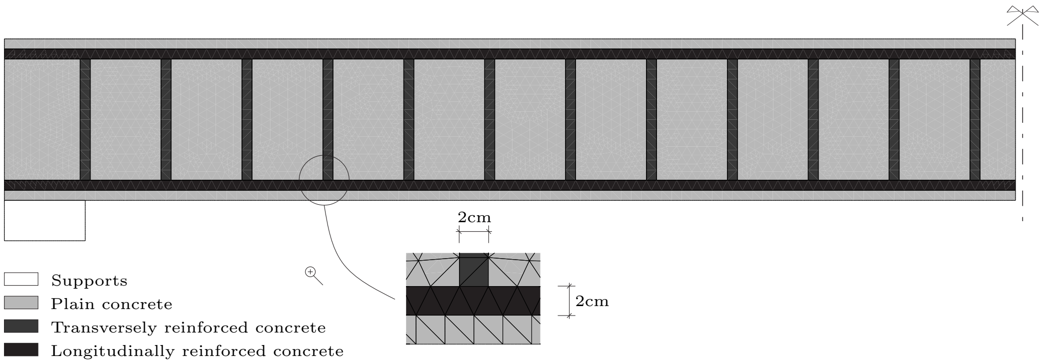

Figure .3: Structural finite element model.

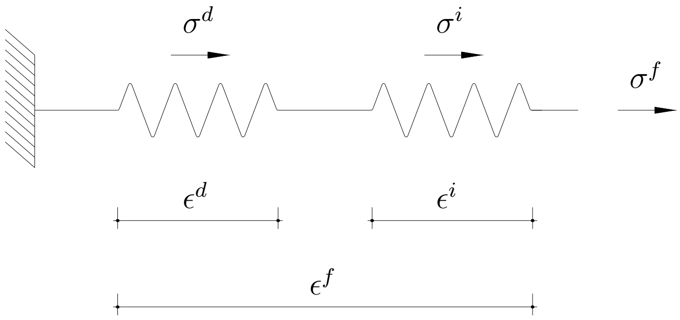

Figure .4: Slipping-fiber model.

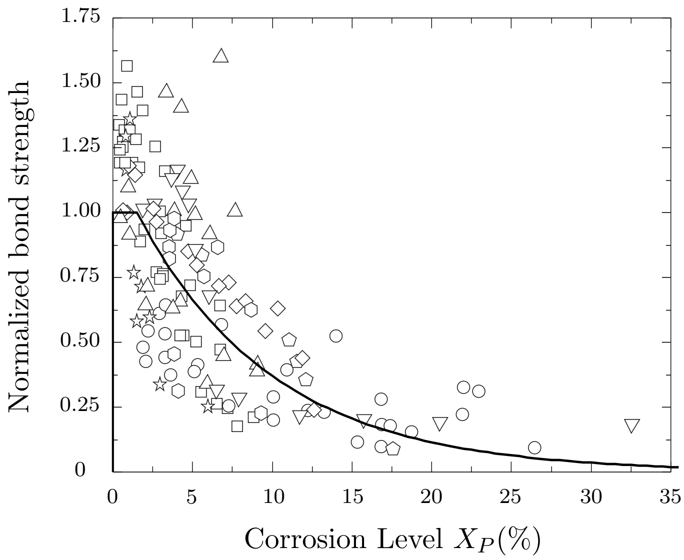

Figure .5: M-pull corrosion-bond model [31].

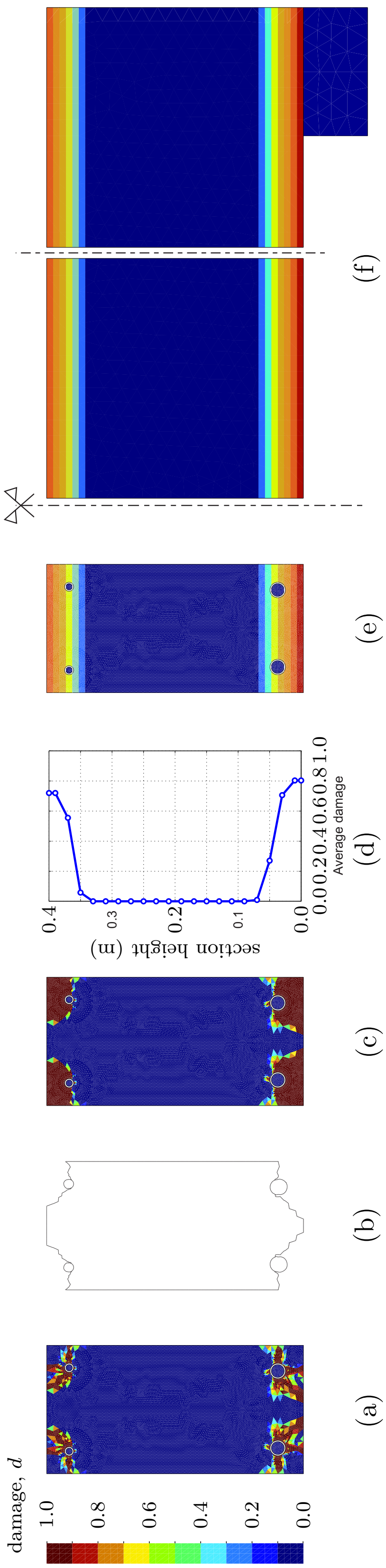

Figure .6: Coupling cross section and structural analysis: (a)concrete damage map, d; (b) effective cross section; (c)equivalent damage distribution; (d) average damage calculation; (e) average damage distribution; (f) initial damage on structural model.

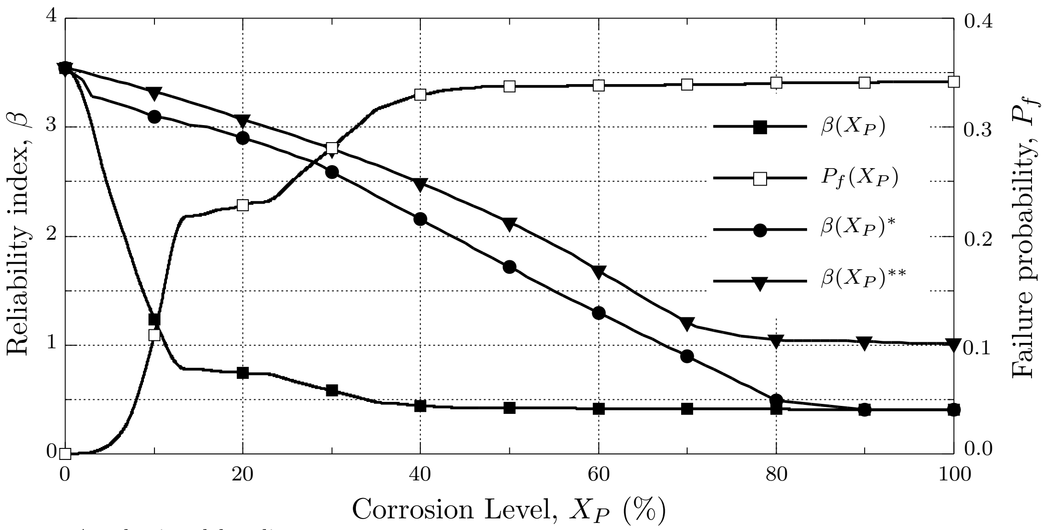

*neglecting debonding
**neglecting debonding and cracking

Figure .7: Reliability index, β, and failure probability, P_f, as a function of the corrosion level, X_P.

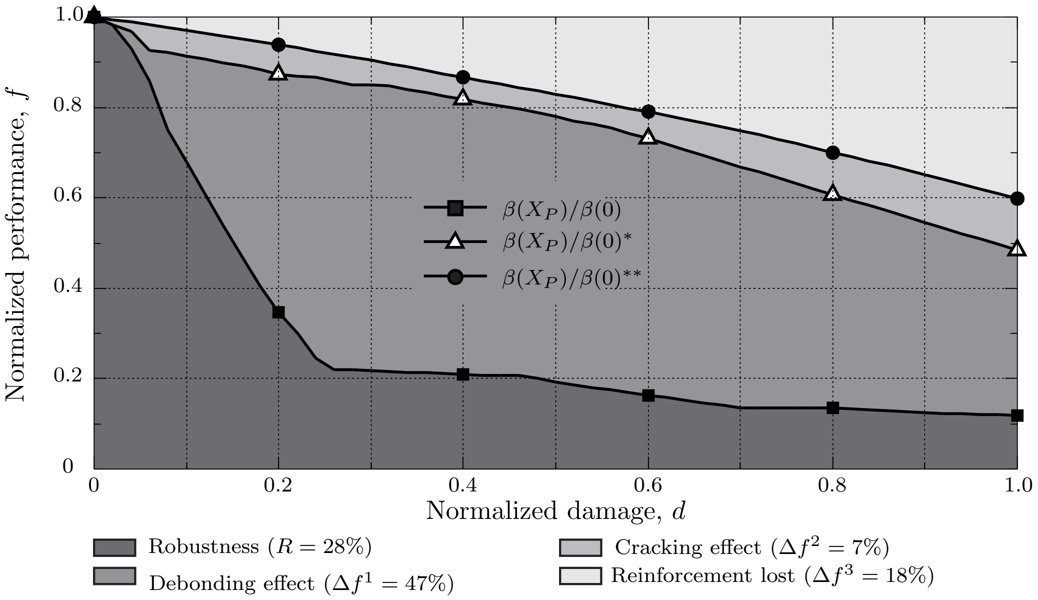

Figure .8: Normalized performance as a function of normalized damage considering: $\beta(X_P)/\beta(0)$, all three deteriorating effects; $\beta(X_P)/\beta(0)^*$, neglecting debonding effect; $\beta(X_P)/\beta(0)^{**}$, neglecting cracking and debonding effects.

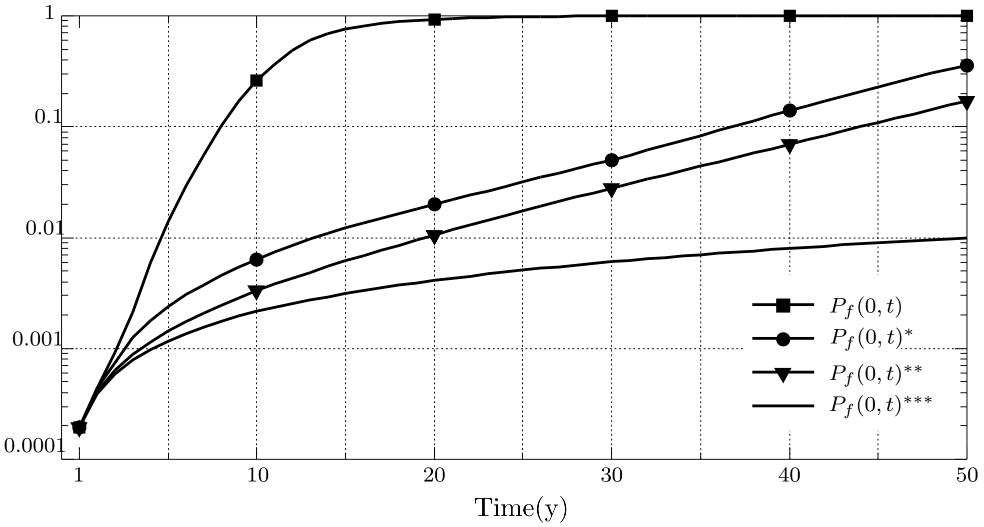

Figure .9: Time-dependent probability of failure considering: $P_f(0,t)$, all three deteriorating effects; $P_f(0,t)^*$, neglecting debonding effect; $P_f(0,t)^{**}$, neglecting cracking and debonding effects; $P_f(0,t)^{***}$, protection against corrosion

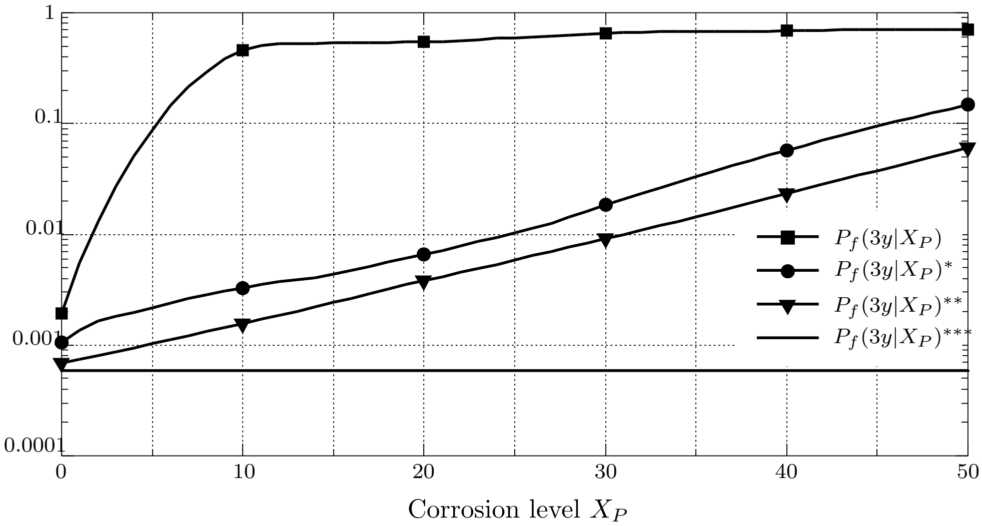

Figure .10: Probability of failure within the period between inspections, considering: $P_f(3y|X_P)$, all three deteriorating effects; $P_f(3y|X_P)^*$, neglecting debonding effect; $P_f(3y|X_P)^{**}$, neglecting cracking and debonding effects; $P_f(3y|X_P)^{***}$, protection against corrosion

List of Tables

Table .1: Random variables distributions and parameters

Random Variable	Dist.	Mean	Std. dev.
Concrete strength, f_c	logn	$38.5MPa$	$5.8MPa$
Steel yield stress, σ_y^i	norm	$460MPa$	$30MPa$
Concrete self-weight, g	norm	$25kN/m^3$	$0.75kN/m^3$
Live loads, q	exp	$0.90kN/m^2$	$0.90kN/m^2$
Resistance model uncertainty, θ_R	logn	1.1	0.15
Load model uncertainty, θ_E	logn	1.0	0.10